

Open channel discharge measurement using the acoustic transit time method – a case study

A. Abgottspon¹, T. Staubli², N. Gloor¹

¹etaeval GmbH, 6048 Horw, Switzerland

²Hochschule Luzern, Technik & Architektur, 6048 Horw, Switzerland

andre.abgottspon@etaeval.ch

Abstract. A case study of discharge measurements with the acoustic transit time method in a rectangular open channel at the intake of the dotation hydro power plant of Pradella, Switzerland is presented. These measurements were performed in the context of efficiency testing of the recently installed turbines. The power plant started operation in 2014 and is equipped with two Kaplan machine groups. The turbines are operated with the residual water fed into the river Inn. By means of the measurements the cam correlation, implemented in the control system, was verified. The results showed that both machine groups are operating close to the envelope determining the on-cam points. Further goal of the measuring campaign was to provide a proof for the required flow rate of the residual water.

The correct extrapolation of the velocity data towards the free surface and the bottom of the open channel was major challenge of the discharge integration. In order to estimate the measurement uncertainty a sensitivity analysis with respect to the chosen extrapolation procedure was carried out. Analysis of the path velocities showed the important influence of the upstream intake structure on the velocity distribution and the fluctuations in the channel. From the difference of the velocities on crossed paths could be concluded that a dominant swirl prevails in the channel.

1. Setup of the installation

The dotation hydro power plant (HPP) Pradella operated by the Engadiner Kraftwerke AG (EKW) provides the residual water, which has to be fed into the river Inn downstream of Pradella, Switzerland. Two vertical Kaplan units are installed with a rated capacity of 450 kW each. The turbines were taken into operation in 2014. The rated head is 10.5 m and the nominal discharge is 5 m³/s for each turbine. In a typical year the annual energy production amounts to 2.9 Mio kWh.

The company etaeval installed temporarily its 8 path acoustic transit time (ATT) equipment in the intake channel (Rittmeyer, Risonic 2000, 1 MHz). Propeller type current meters were considered not to be adequate due to the expected swirl in the measuring section. Figures 1 to 3 depict the intake structure and the setup of the measurements. The water is fed at an angle of 90 deg. from the main channel underneath a wall into the intake channel. Shortly afterwards an other 90 deg. bend follows. After that a straight section of the open channel follows, before the channels widens and feeds the trash racks of the two machine groups (MG).

The prevailing flow features are schematically sketched in figure 2 and 3. The light blue line indicates a possible path of a streamline in the center flow and the dashed dark blue indicates the superimposed rotation of the flow.

The open channel has a width of 3.214 m and the mean water depth was 3.331 m at the position of the measuring section. The ATT installation consists of two crossed planes, four layers and eight acoustic paths. The measuring cross section, the transducer positions and the angles were individually measured for every path using a total station. The free surface levels in the channel (high pressure measuring section) and after the draft tube outlet (low pressure measuring section) were measured with ultrasonic sensors. Further measurement equipment (power meter, pressure transducers and regulating position measurements) were installed inside the turbine building.

The data acquisition rate for all signals was 1 Hz. The path velocities were determined from the measured acoustic transit times acquired at this rate. The discharge data were then evaluated by integration of the individual path velocities. The estimation of the amount of the required data points to get a small random uncertainty prior the test was estimated to be 360 samples (which corresponds to an acquisition duration of 6 minutes). Due to high scatter of the efficiency data and low frequency fluctuation of discharge it was decided during the test to increase the number to 600 samples (10 minutes). Outliers were removed on the basis of the Grubbs test [1].

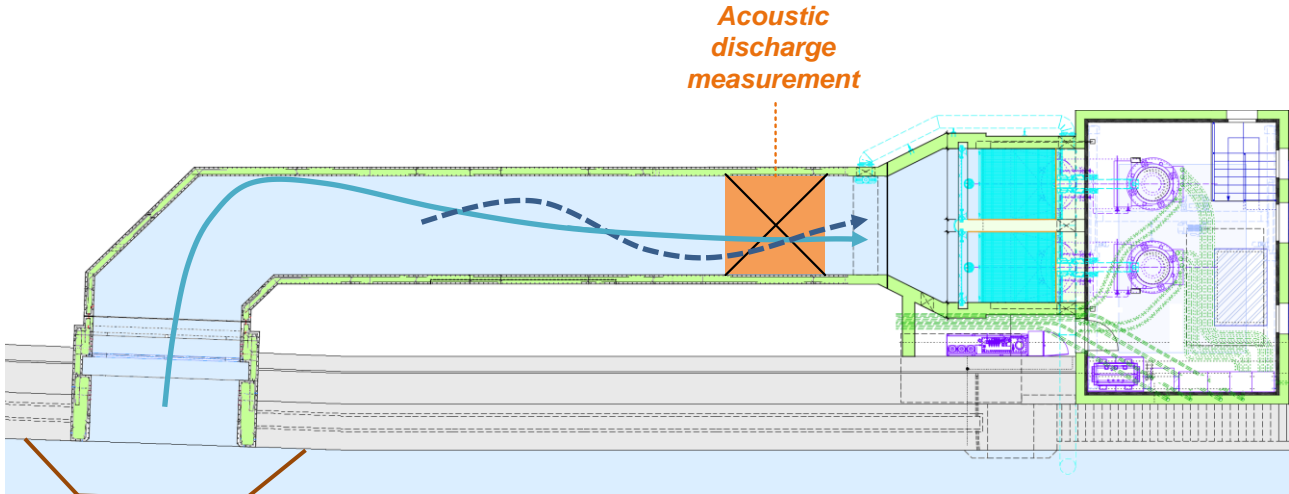


Figure 1. Top view of the dotation HPP Pradella.

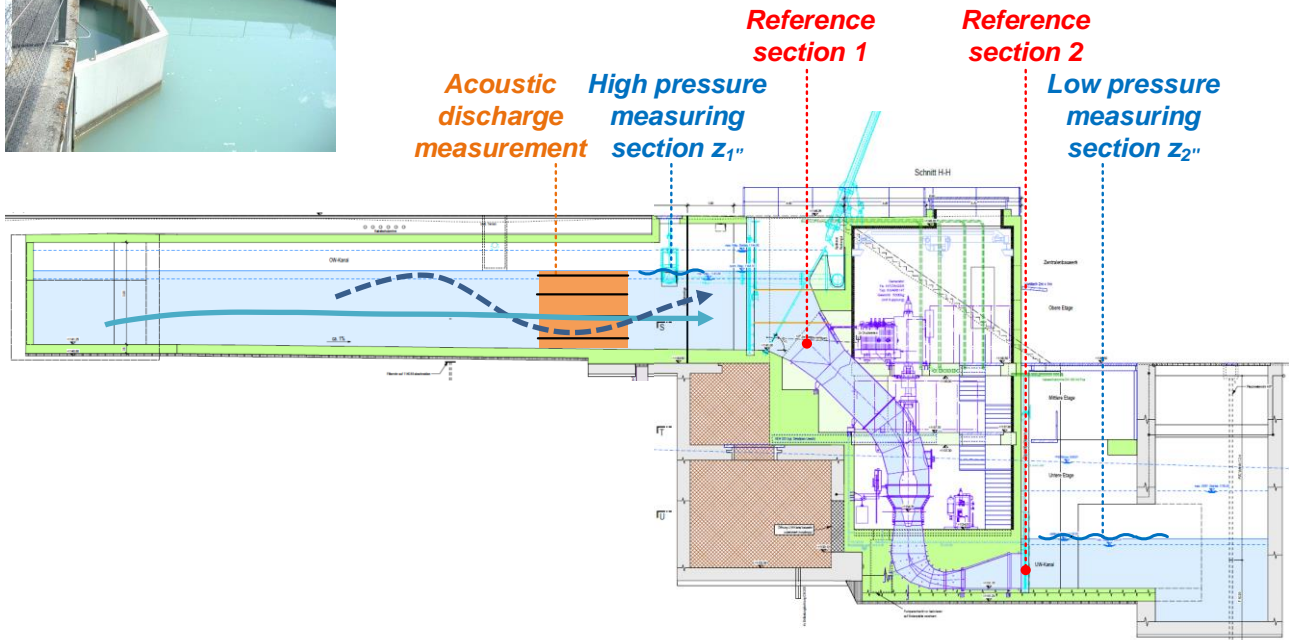


Figure 2. Side view of the dotation HPP Pradella with a schematic of the flow in the open channel.

In order to avoid signal reflections on the bottom or the surface of the channel, the lowest and highest path positions (layer 1 and 4 according to figure 3) have to be chosen so that the distance from bottom and surface does not fall below an allowed limit. For the calculation of the minimum distance from the free water surface the following estimation can be used

$$z_{\min} \approx 60 \cdot \sqrt{\frac{L}{f}} = 60 \cdot \sqrt{\frac{4.439m}{1 \cdot 10^6 Hz}} = 0.13m \quad (1)$$

z_{\min} Minimum distance from the free water surface [m]

L	Path length	[m]
f	Transducer frequency	[Hz]

A more detailed derivation of the distance is given by Lanzersdorfer [2]. In our case it was advantageous that the free water level was constant and the surface smooth. For the positioning of the lowest layer the manufacturer recommends a minimum distance between 0.2 and 0.3 m from the channel bottom. For the measurement setup at the dotation HPP Pradella the layer 1 was installed at a height of 0.3 m above the channel bottom and the layer 4 at a height of approximately 0.3 m below the free surface.

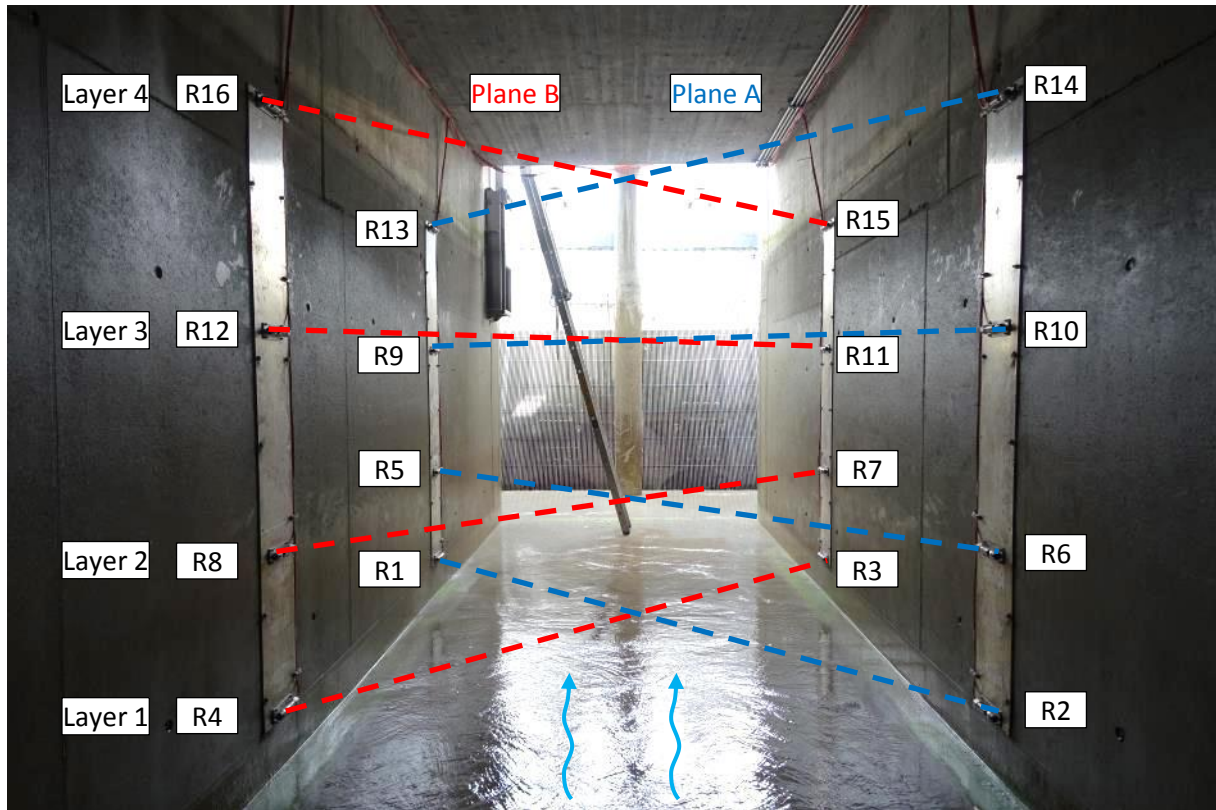


Figure 3. ATT installation within the rectangular open channel.

The value of the free surface level is required to calculate the flow area. This level was not measured exactly at the same position as of the ATT installation. Therefore the backwater curve had to be taken into account. The amount of this influence was estimated to be 0.002 m, which is 0.06 % of the mean water height of 3.331 m, thus this influence can be neglected.

The nomenclature and the calculation of the mean axial and the transversal velocities on each layer used in this paper follow the contribution of Hug et al. [3]. The ISO Standard 6414 [4] describes general principles of the ATT method and the ISO Standard 748 [5] deals with the discharge integration in open channels.

2. Velocity profiles

Figure 4 shows the measured velocity profiles of the velocity components in axial and transversal directions. The graphs on the left side display the velocities in m/s and the graphs on the right side show the velocities non-dimensionalized with the mean axial velocity (discharge divided by flow area). The four layers and the free water surface level are indicated by dashed lines. The lines corresponding to each measured propeller curve (figure 13) have the same color. The mean discharge values for each propeller curve measurement are given below the diagrams of figure 4.

The observed axial flow profile is rather unusual; one would not expect the highest velocities close to the channel bottom. The higher the discharge the steeper the flow profile becomes, but the shape of axial flow profile is changing only little with the discharge. The maximum axial velocity is always measured on the lowest layer.

All transversal velocity profiles show a zero crossing point on approximately half-height of the channel. Since the vertical velocity gradients of the transversal velocity are constant for each operating point it can be

concluded that a rigid body rotation of the water exists. Such a rotation of the channel flow prevails over the entire operating range, but its strength increases almost linearly with the flow rate. Furthermore, the ratio of the transversal velocity to the mean axial velocity amounts up to 25 % near the surface.

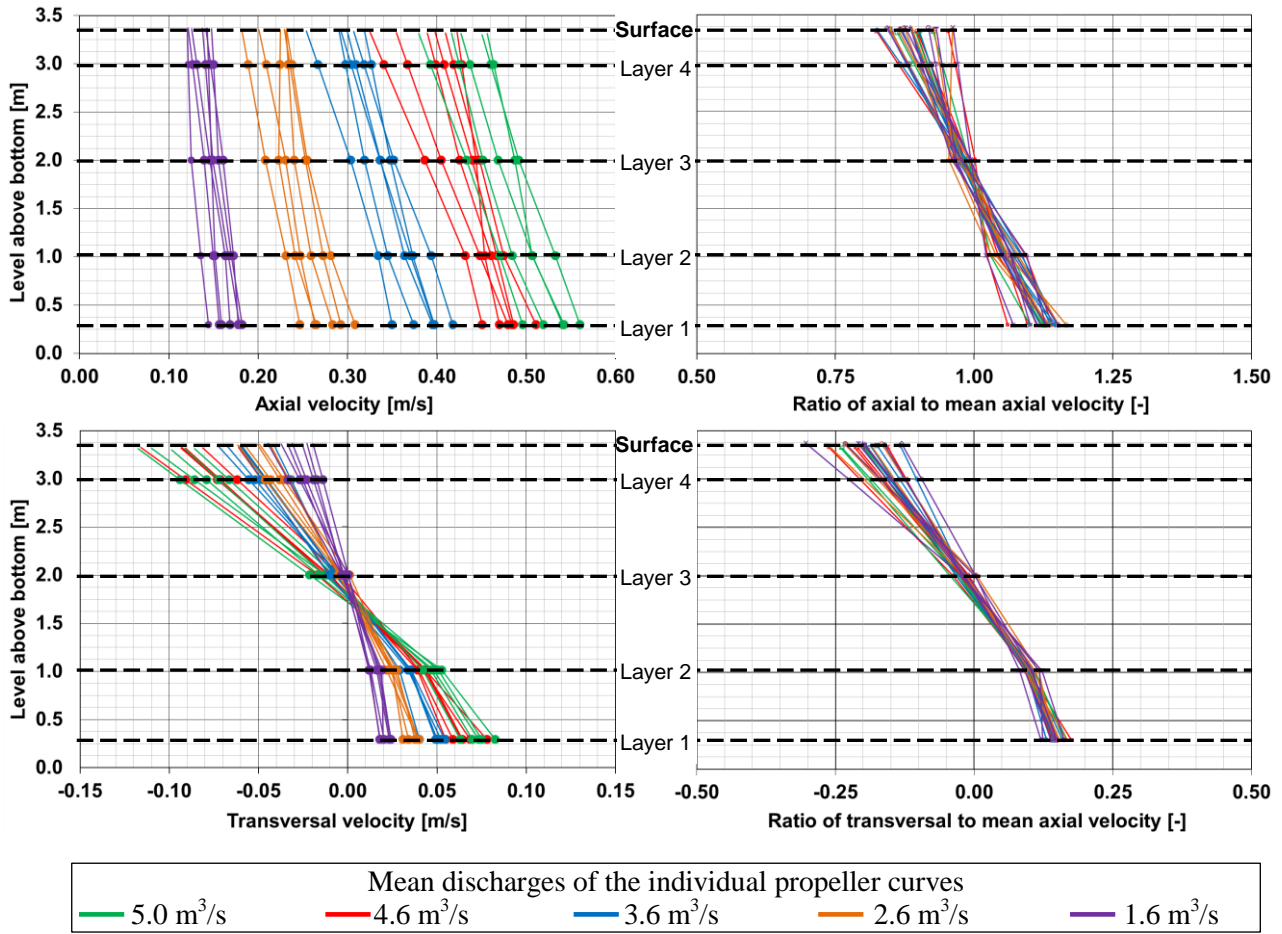


Figure 4. Measured axial and transversal velocity components with linearly extrapolated surface velocities.

Figure 5 shows the time signal of the angular velocity for a typical measuring point. This angular velocity is derived from the mean gradient of the transversal velocity:

$$\omega = \frac{v_{tr}}{r} \quad (2)$$

ω	Angular velocity	[rad/s]
v_{tr}	Transversal velocity	[m/s]
r	Radius from the centre of rotation	[m]

The rotation can be evaluated from the time mean data as shown in figure 4, but also from the instantaneous gradients of the transversal velocities. The temporal fluctuations of the angular velocity for one selected measuring point with a mean axial velocity of 0.34 m/s are displayed in figure 5. The mean value of the angular velocity is at 0.04 rad/s, while the peak-to-peak values reach 0.08 rad/s. These observed low frequency fluctuations lead to statistically not independent acquisition of data points and might give the explanation for the scatter of the mean discharge values and the non-satisfying repeatability.

A propeller type current meter exposed to such a rotating flow will read too high or too low velocities depending on the sense of rotation. For the case of the example shown in figure 5 a common OTT C31 R-type current meter, which has 4 revolutions per meter in the towing tank, will rotate at an angular velocity of 8.55 rad/s at the velocity of 0.34 m/s. Thus the angular velocity of 0.04 rad/s of the flow rotation will lead to an error of 0.55 % of the speed of rotation of the current meter. Since all current meters in a measuring section will be exposed to approximately the same angular velocity a systematic error of the discharge of the same order will result.

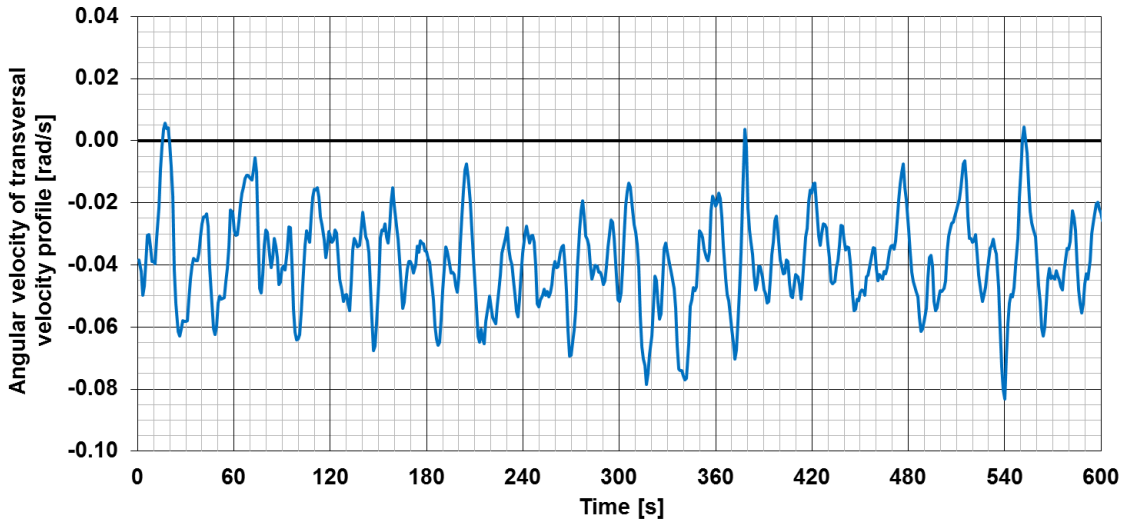


Figure 5. Mean angular velocity of the flow due to the transversal velocities for one measuring point.

3. Discharge calculation

The total discharge is calculated from the four measured mean axial velocities on the four layers and from an estimation of the velocity profiles above the highest layer and below the lowest layer. The estimation of the discharge above the highest layer is called Q_{surf} and the one below the lowest layer Q_{bot} . In literature different approaches to calculate Q_{surf} and Q_{bot} can be found. In order to evaluate the sensitivity of the discharge on the different assumptions some of methods were applied and their results compared.

$$Q = Q_{bot} + Q_{int} + Q_{surf} \quad (3)$$

Q	Total discharge	$[m^3/s]$
Q_{bot}	Bottom discharge	$[m^3/s]$
Q_{int}	Intermediate discharge	$[m^3/s]$
Q_{surf}	Surface discharge	$[m^3/s]$

3.1. Surface discharge

Method 1: Linear extrapolation (ISO 6416)

In this method the surface velocity is determined on the basis of a linear extrapolation. In our case the velocity was extrapolated from the layer velocities v_3 and v_4 . Furthermore, a site-specific surface coefficient is introduced in this method. Q_{surf} can then be calculated as follows:

$$Q_{surf} = \frac{v_4 + (k_{surf} \cdot v_{surf})}{1 + k_{surf}} \cdot (z_{surf} - z_4) \cdot \frac{B_4 + B_{surf}}{2} \quad (4)$$

and

$$v_{surf} = v_4 + \left(\frac{v_4 - v_3}{z_4 - z_3} \right) \cdot (z_{surf} - z_4) \quad (5)$$

v_{surf}	Axial velocity of the surface	$[m/s]$
v_4	Axial velocity of the layer 4	$[m/s]$
k_{surf}	Surface coefficient	$[-]$
z_{surf}	Height of the water surface	$[m]$
z_4	Height of the layer 4	$[m]$
B_{surf}	Channel width at the water surface	$[m]$
B_4	Channel width at the layer 4	$[m]$

Method 2: Exponential extrapolation (Giordano)

The method developed by Giordano [7] calculates Q_{surf} with the approximated surface velocity and highest layer velocity.

$$Q_{surf} = \frac{v_4 + v_{surf}}{2} \cdot (z_{surf} - z_4) \cdot \frac{B_4 + B_{surf}}{2} \quad (6)$$

The surface velocity results from the multiplication of the highest measured axial velocity with the surface coefficient.

$$v_{surf} = k_{surf} \cdot v_4 \quad (7)$$

The surface coefficient, which corresponds to an area-ratio, is calculated from the highest measured axial velocity and the extrapolated surface velocity. In the case of the presented measurements the surface coefficient results to 0.972.

$$k_{surf} = \frac{v_{z0.99}}{v_{z0.9}} \quad (8)$$

$v_{z0.99}$	Standardized velocity at 99 % of the water level	[-]
$v_{z0.90}$	Standardized velocity at 90 % of the water level	[-]

The velocity profile below the water surface is approximated with an exponential function. The parameters v_{G3} , n_3 and k_3 specify the form of the velocity profile. With the following function the velocity profile is extrapolated:

$$v(z) = v_{G3} \cdot z^{\frac{1}{n_3}} \cdot e^{\frac{-k_3 \cdot z}{n_3}} \quad (9)$$

$v(z)$	Axial velocity in function of the height	[m/s]
z	Height above channel bottom	[m]
v_{G3}	Velocity standardizing coefficient	[-]
n_3	Inclination coefficient	[-]
k_3	Geometry coefficient	[-]

The geometry factor is determined by:

$$k_3 = \frac{\frac{28}{3}}{\frac{7}{3} + \frac{B}{z_{surf}}} \quad (10)$$

B	Mean channel width	[m]
-----	--------------------	-----

The hydraulic radius in a rectangular channel is derived from:

$$R_h = \frac{B \cdot z_{surf}}{B + 2 \cdot z_{surf}} \quad (11)$$

R_h	Hydraulic radius	[m]
-------	------------------	-----

The coefficient to calculate the inclination coefficient is calculated by:

$$n_i = \frac{k_{Karm} \cdot R_h^{\frac{1}{6}} \cdot K_s}{\sqrt{g}} \quad (12)$$

n_i	Coefficient	[-]
k_{Karm}	Kármán constant	[-]
K_s	Gaukler-Strickler coefficient	$[m^{1/3}s^{-1}]$
g	Gravitational acceleration	$[m/s^2]$

The inclination coefficient depends on the geometry factor and is determined by:

$$n_{3(k_3>1)} = n_i \cdot 0.7 \quad (13)$$

$$n_{3(0<k_3<1)} = n_i \cdot (1 - k_3 \cdot 0.3) \quad (14)$$

With this, the velocity standardizing coefficient is derived from:

$$v_{G3} = (k_3 \cdot e^1)^{\frac{1}{n_3}} \quad (15)$$

3.2. Intermediate discharge

The calculation of the discharge between the lowest and the highest layers is carried out according to the ISO Standard 6416 (mean-section method).

$$Q_n = \frac{v_n + v_{n+1}}{2} \cdot (z_{n+1} - z_n) \cdot \frac{B_n + B_{n+1}}{2} \quad (16)$$

Q_n	Discharge of one channel cross-section	$[m^3/s]$
B_n	Channel width of the corresponding layer	[m]
z_n	Height of the corresponding layer	[m]
v_n	Axial velocity of the corresponding layer	[m/s]

3.3. Bottom discharge

Method 1: Mean section method (ISO 6416)

The discharge of the lowest channel cross-section is calculated according to the ISO Standard 6416 (mean-section method) as follows:

$$Q_{bot} = \frac{1 + k_{bot}}{2} \cdot v_1 \cdot (z_1 - z_{bot}) \cdot \frac{B_{bot} + B_1}{2} = K_{bot} \cdot v_1 \cdot (z_1 - z_{bot}) \cdot \frac{B_{bot} + B_1}{2} \quad (17)$$

With the substitution:

$$K_{bot} = \frac{1 + k_{bot}}{2} \quad (18)$$

The mean axial velocity of the lowest channel cross-section is:

$$\frac{1 + k_{bot}}{2} \cdot v_1 = K_{bot} \cdot v_1 \quad (19)$$

Q_{bot}	Discharge of the lowest channel cross-section	$[m^3/s]$
v_1	Axial velocity of the layer 1	[m/s]
k_{bot}	Bottom coefficient	[-]
z_1	Height of the layer 1	[m]
z_{bot}	Height of the bottom	[m]
B_1	Channel width at the layer 1	[m]
B_{bot}	Channel width at the bottom	[m]

The calculation of the bottom coefficient is not specified in the Standard. Though, it can be determined with the common power law. The bottom coefficient is described in the ISO Standard 6416 to be usually between

0.4 and 0.8.

$$v_1 = v_2 \cdot \left(\frac{z_1}{z_2} \right)^n \quad (20)$$

n Exponent [-]

$$\text{Therefore } n = \frac{\ln\left(\frac{z_2}{z_1}\right)}{\ln\left(\frac{v_2}{v_1}\right)} \quad (21)$$

With this exponent, the bottom coefficient yields to:

$$k_{bot} = \frac{2 \cdot n}{n + 1} - 1 \quad (22)$$

A bottom coefficient k_{bot} of 0.4 means a fast increasing axial velocity with increasing distance from the bottom and a bottom coefficient of 0.8 means a slowly increasing axial velocity in the lowest channel cross-section. However, in the presented case the described way to calculate the bottom coefficient is not applicable, since the highest velocity is measured on layer 1 and the bottom coefficient would be larger than 1 (see table 1). Consequently, the bottom velocity is increasing near to the bottom, what is not realistic. This method can only be recommended for increasing axial velocities between the layer 1 and the layer 2.

z_1	z_2	v_1	v_2	n	k_{bot}	v_{bot}
[m]	[m]	[m/s]	[m/s]	[-]	[-]	[m/s]
0.1	0.3	0.5	0.45	-10.4	1.21	0.6

Table 1. Example calculation of the bottom coefficient in the case of the dotation HPP Pradella.

Method 2: Exponential extrapolation (Giordano)

The axial velocity is calculated according to the exponential extrapolation method from the measured axial velocity at the lowest layer. The discharge of the lowest channel cross-section is calculated as follows:

$$Q_{bot} = K_{bot} \cdot v_1 \cdot (z_1 - z_{bot}) \cdot \frac{B_{bot} + B_1}{2} \quad (23)$$

This is the same approach as used for method 1. The mean axial velocity of the lowest channel cross-section is:

$$K_{bot} \cdot v_1 \quad (24)$$

The bottom coefficient is found by the integration of the velocity profile from the channel bottom to the first measured layer velocity. It is the same procedure as the exponential extrapolation of the surface velocity. The bottom coefficient corresponds to an area-ratio.

$$K_{bot} = \frac{\int_{z_{bot}}^{z_1} v(z) \cdot dz}{z_{1_standardized} \cdot v_{1_standardized}} \quad (25)$$

K_{bot} Bottom coefficient [-]

In the presented case the extrapolated velocity profile near the bottom becomes too flat with the Giordano method and results in a bottom coefficient K_{bot} of 0.976. Converted into a bottom coefficient k_{bot} according to

the ISO Standard 6416 gives $k_{bot} = 0.95$, larger than an expected value of 0.4 to 0.8. Therefore, the resulting mean axial velocity in the lowest channel cross-section with this method becomes too high.

Method 3: Velocity distribution method (ISO 748)

Another way to determine the velocity profile is with the velocity distribution method described in the ISO Standard 748. This method is only appropriate for increasing velocities between the layer 1 and layer 2, what is not the case here. The discharge of the channel cross-section is calculated as follows:

$$Q_{bot} = K_{bot} \cdot v_1 \cdot (z_1 - z_{bot}) \cdot \frac{B_{bot} + B_1}{2} \quad (26)$$

The mean axial velocity of the lowest channel cross-section is:

$$K_{bot} \cdot v_1 \quad (27)$$

The bottom coefficient is:

$$K_{bot} = \left(\frac{m}{m+1} \right) \quad (28)$$

m Coefficient for the roughness of the bottom [-]

The coefficient of roughness described in the ISO Standard 748 reaches from 4 (rough surface) to 10 (smooth surface). Applied on the bottom coefficient K_{bot} it gives a value range of 0.8 to 0.91.

The bottom coefficient can be calculated as well as from the integration of the velocity profile on the basis of equation (25). The integration is set between the channel bottom and the first measured layer and gives a bottom coefficient K_{bot} of 0.9. Converted into a bottom coefficient k_{bot} according to the ISO Standard 6416 gives $k_{bot} = 0.8$. A possible resulting velocity profile in the lowest channel cross-section according to a K_{bot} factor of 0.9 (or of k_{bot} factor of 0.8) is depicted in figure 6. The calculated velocity profile (red) is designed according to the power law:

$$v(z) = v_a \cdot \left(\frac{z}{z_a} \right)^{\frac{1}{m}} \quad (29)$$

This is the same approach as in equation (20), but with a different exponent.

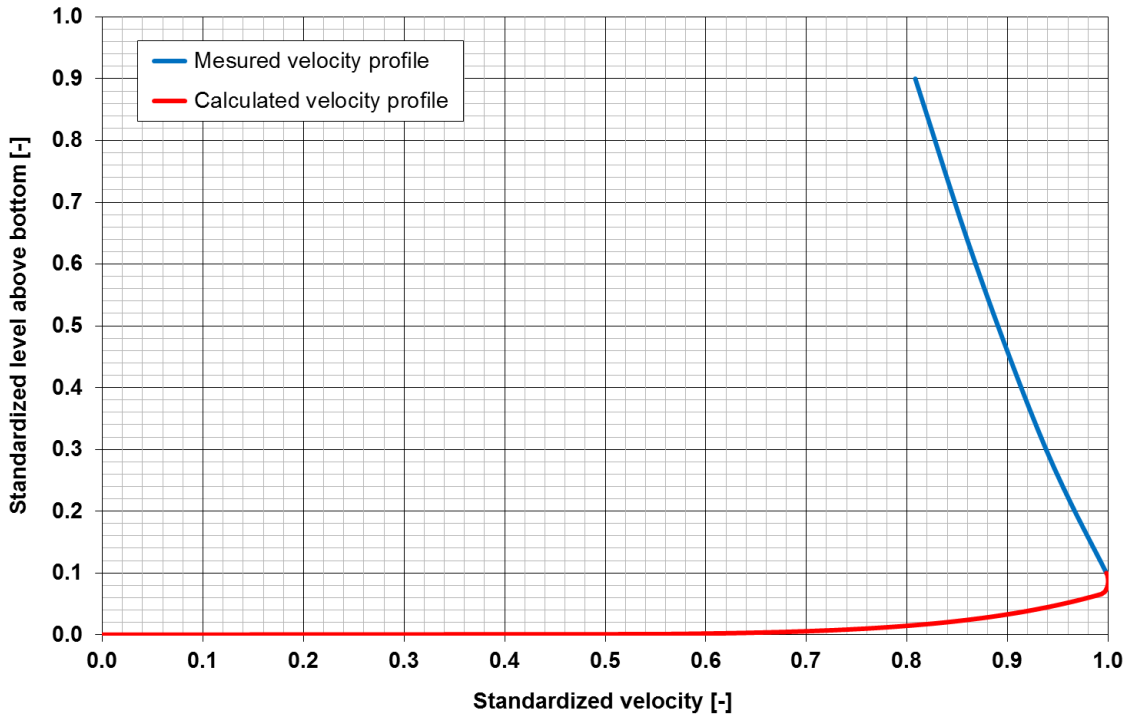


Figure 6. Extrapolation of the bottom axial velocity with $K_{bot} = 0.9$.

4. Comparison of different extrapolation methods

For the discharge calculations at the dotation HPP Pradella the following methods were used

- surface discharge: exponential (Giordano)
- intermediate discharge: mean-section method (ISO 6416)
- bottom discharge: velocity distribution method (ISO 748)

Figure 7 shows the resulting deviations of different methods for the calculation of the surface and bottom discharge in percent of the total discharge. The differences between the two methods for the calculation of the surface discharge are marginal. The differences between the exponential extrapolation and the velocity distribution method for the calculation of the bottom discharge are with 0.75 % important. With the graphical based estimation in dependence on the exponential extrapolation of Giordano it becomes obvious, that the velocities near the channel bottom are too high and therefore the reduction to a zero velocity on the bottom is not physical or too flat. The difference of 0.75 % corresponds to the resulting K_{bot} factor of 0.9 according to the velocity distribution method and the K_{bot} factor of 0.976 according to the exponentially extrapolation method. For this reason the differences between the methods do not depend on discharge.

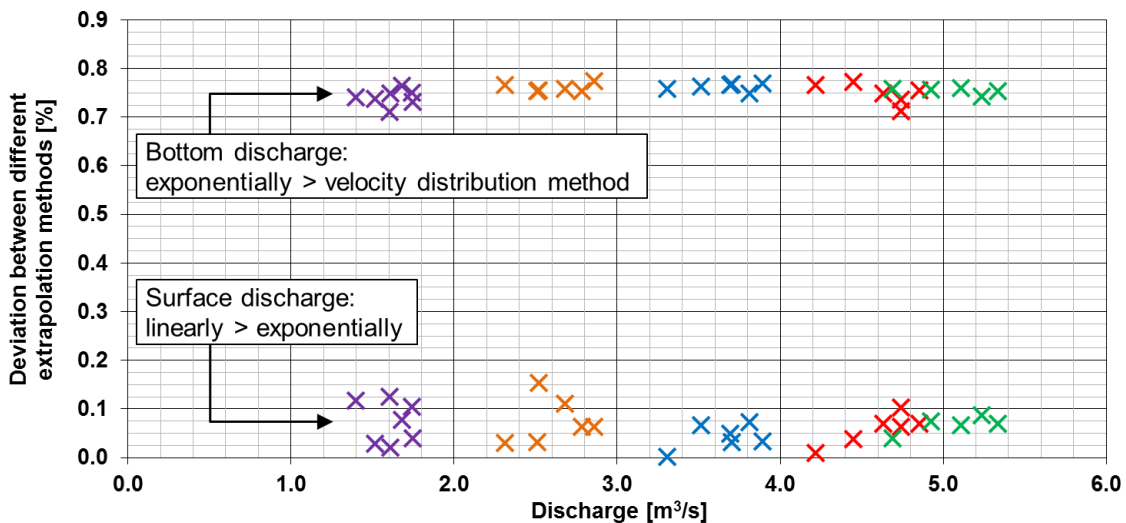


Figure 7. Influence of the extrapolation method for the surface and bottom velocities on the discharge.

5. Analysis of the discharge signals

Figure 4 in section 2 shows that a dominant rotation of the flow or swirl is present in the measuring section. Therefore, a crossed path installation is mandatory. In Figure 8 the individual flow rates of plane A and B are depicted over the measured discharge range. Furthermore, the deviation of the single flow rates from plane A and B to the mean discharge in percent is added to the figure at the secondary axis. At the beginning of the measurement campaign the acquisition duration for one measuring point was set to 360 s. Due to the unusual scatter of the mean data it was then decided to increase the acquisition duration to 600 s. It can be observed in figure 8 that the deviations become slightly lower with the longer acquisition duration. A configuration without crossed paths would result in an under- or overestimation of the discharge of up to 3 % (the mean value is 1.4 %).

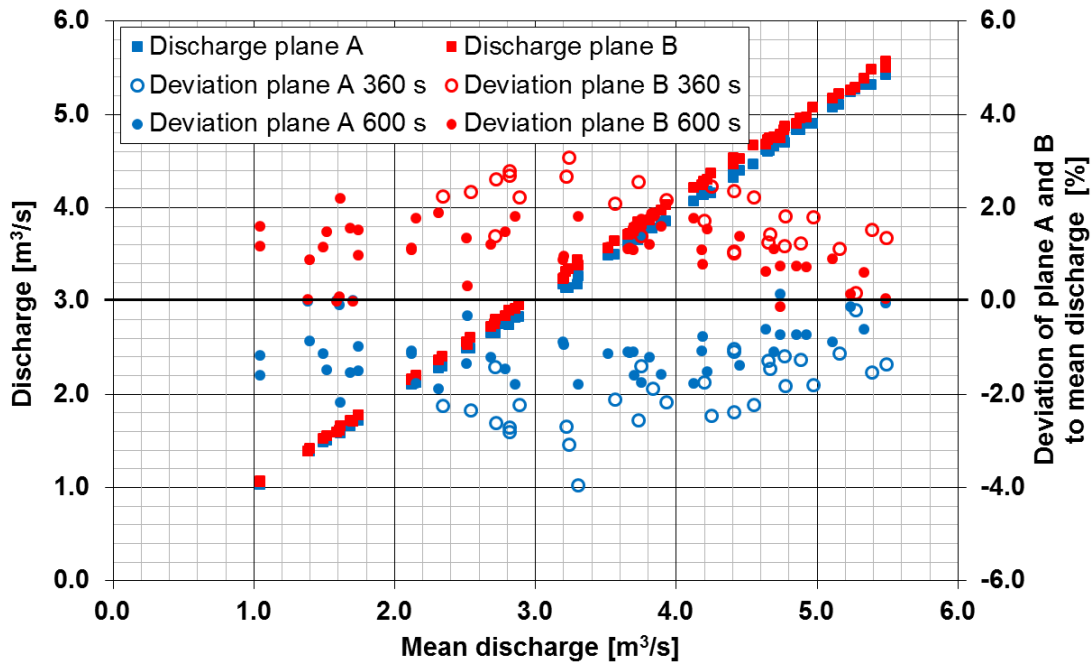


Figure 8. Discharge and deviation of planes A and B for all measuring points.

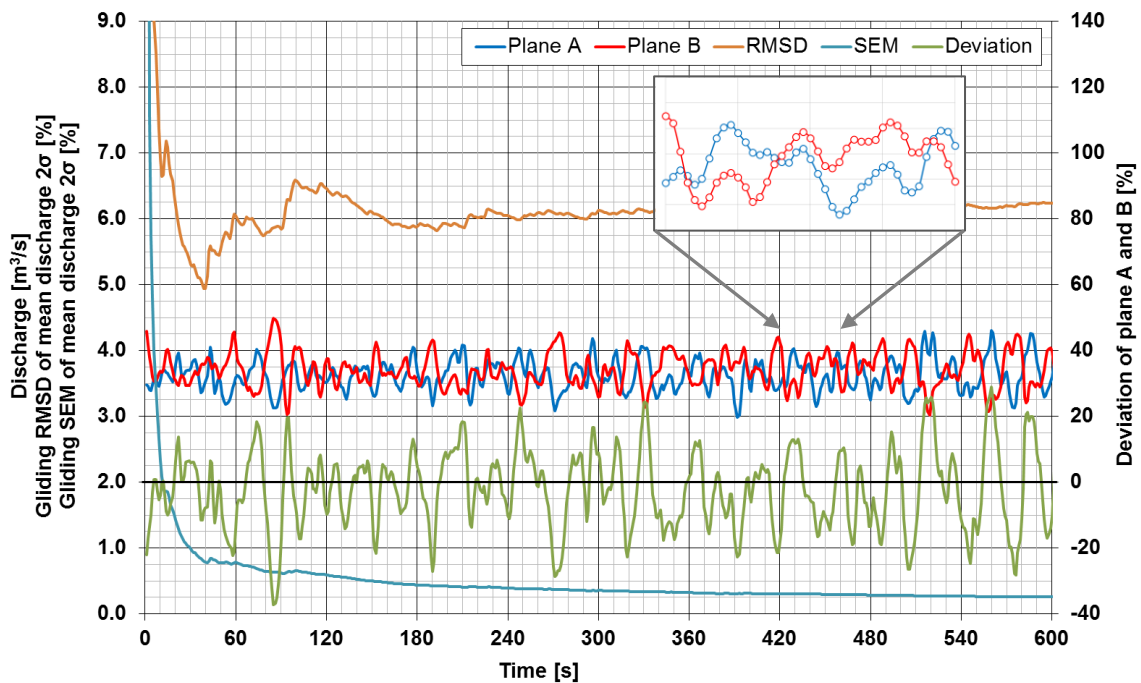


Figure 9. Discharge, statistics and deviation of planes A and B for one measuring point.

Figure 9 shows a time signal of a measuring point with an acquisition duration of 600 s. The individual flow rates of the planes A and B are shown scaled with the primary axis. The deviations in percent between these two discharges are shown with the secondary axis. The statistical data (root-mean-square deviation = RMSD and standard error of the mean = SEM) of the mean discharge are also scaled with the primary axis. The statistical data are given for a confidence interval of 95 %. In a zoom view of 40 s the low frequency fluctuation of the discharge signals are shown. With the acquisition rate of 1 Hz the fluctuations are well resolved, but the samples are statistically dependent.

If the discharge fluctuations are in phase in plane A and B, then this is a sign of longitudinal fluctuations of the flow in the channel. On the other hand if a positive peak in the time signal of plane A corresponds to a negative peak in the time signal of plane B, this is an indication for a fluctuation of the transversal velocities, thus in the present case of the swirl. These fluctuations of the transversal velocities cause the deviations between plan A and B and are therefore a reason for the scatter of the data in figure 8. The RMSD becomes constant after a sufficient number of data for the mean discharge and approaches approximately $\pm 6\%$ for this measuring point. Also the SEM tends to a constant value after 300 s.

Figure 10 shows the auto power spectrum for the same measuring point. The individual flow rates of the planes A and B are depicted in the upper diagram. The spectrum for the mean discharge is shown in the lower diagram. Low frequency fluctuations below 0.1 Hz are observable in the individual spectra of each plane. These fluctuations do not appear in the mean discharge indicating that the fluctuations in the individual planes arise mostly from the transversal velocity fluctuations. The only remaining frequency in the mean discharge is around 0.092 Hz (10.9 s). This frequency corresponds to a surge and sink wave frequency, which develops in the open channel due to discharge variations. The speed of this long waves propagating in a channel can be assumed with:

$$c = \sqrt{h \cdot g} = \sqrt{3.331m \cdot 9.8044 \frac{m}{s^2}} = 5.71 \frac{m}{s} \quad (30)$$

c	Propagation speed	[m/s]
h	Water height	[m]
g	Gravity	[m/s ²]

The mean velocity in the open channel is more than ten times smaller than the propagating velocity and therefore negligible. The open channel has a length of approximately 30 m. This gives 5.3 s for the wave to travel from one end to the other. It can be concluded from this approximation, that such surge and sink waves have a period of 10.6 s in the open channel. This agrees well with the frequency observed in the spectrum of the mean discharge with a period of 10.9 s.

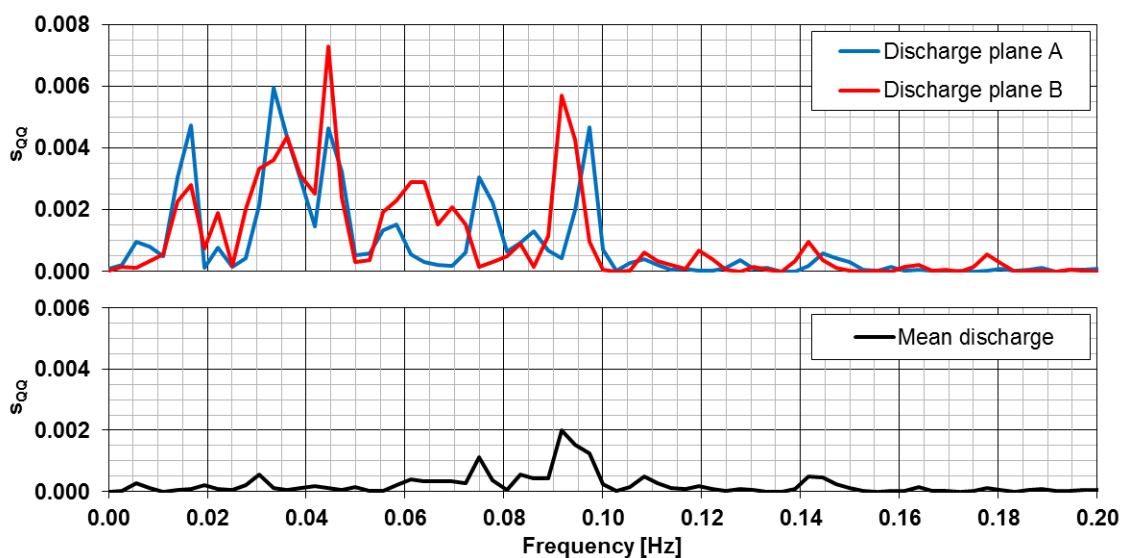


Figure 10. Auto power spectrum analysis for one measuring point.

Figure 11 shows two typical auto correlations of the discharge in plane A for the two different acquisition durations. The calculation of statistics in figure 9 is based on the concept that the acquired data are statistical

independent. However the low frequency components in the signals, which are much lower than the sampling frequency of 1 Hz, lead to the fact that the individual samples are not statistically independent. These low frequencies seem to vary stochastically as can be concluded from the power spectra and also from the auto correlation. While for the shorter acquisition duration some periodicity can be observed in the auto correlation, this periodicity disappears for the longer acquisition duration.

For all the measured data (samples) used for the mean discharge calculation a chi-square test was executed. These data are normally distributed, what allows the conclusion that the amplitudes and the frequencies of the low frequency components vary in a stochastically manner, what is typical for turbulent flows. Furthermore, the skewness and the kurtosis of all the measured samples were analysed with the probability density functions and no irregularities were found.

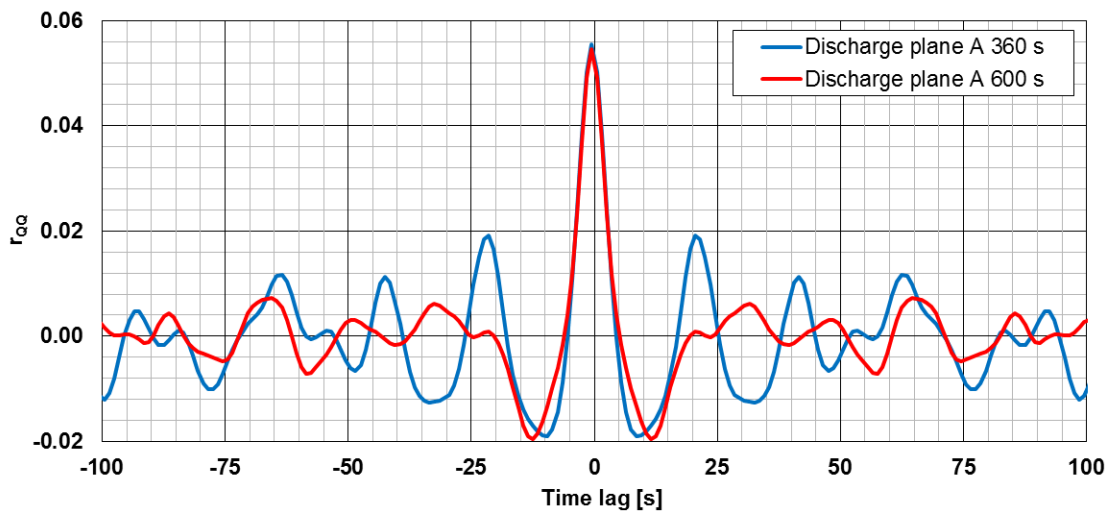


Figure 11. Auto correlation of the discharge in plane A for different acquisition durations.

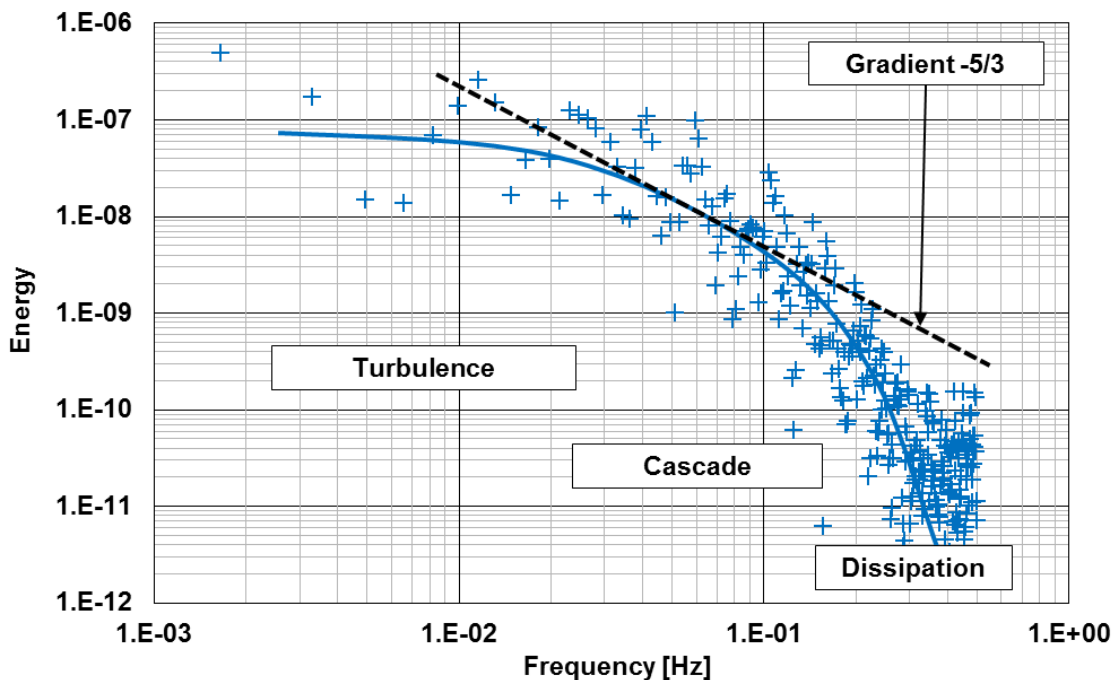


Figure 12. Example of turbulence spectra of measured axial velocity for one path.

Stochastically varying low frequency components are typical for open channel flows, as investigated e.g. by Blanckaert [7]. The larger the channel dimensions are the more energy content can be found at the low frequencies. Figure 12 shows a double logarithmic presentation of the energy spectrum evaluated from the data of one acoustic path. The first frequency point at 0.00167 Hz corresponds to the duration of data acquisition of 600 s. The energy of the fluctuations remain constant up to a frequency of about 0.04 Hz. For

higher frequencies a typical decay of $-5/3$ is observed. The steeper slope at the high frequency end of the graph could be eventually explained by the dissipation of the turbulent structures.

6. Cam correlation test

In addition to the efficiency acceptance tests also the cam correlation (CC) were tested. For such a cam test several propeller curves were measured covering the entire operating range (see figure 13). A single propeller curve results from measuring points with a constant runner blade position and varying guide vane positions. In a next step an envelope efficiency curve is fitted on the different propeller curves. The envelope touches the propeller curve tangentially. The envelope characterizes the optimum points of operation at a given head and for different loads. The procedure of CC tests is described in detail in the Annex I in the IEC Standard 62006 [8].

Figure 13 shows the results for the MG 1 which are quite similar to the results of MG 2. The results show that both machine groups are operating close to the envelope for the on-cam points. Minor corrections of the CC will be implemented in the control system.

Furthermore, the resulting discharge for every guide vane position was implemented in the control system according to the efficiency test results. Based on the results measured at one head, extrapolations of the optimal CC curve for other heads were calculated. With this set of data, the discharge will be used in future for regulating purposes of the main weir next to the dotation HPP Pradella and to control the contractual residual water for the river Inn downstream of the main weir.

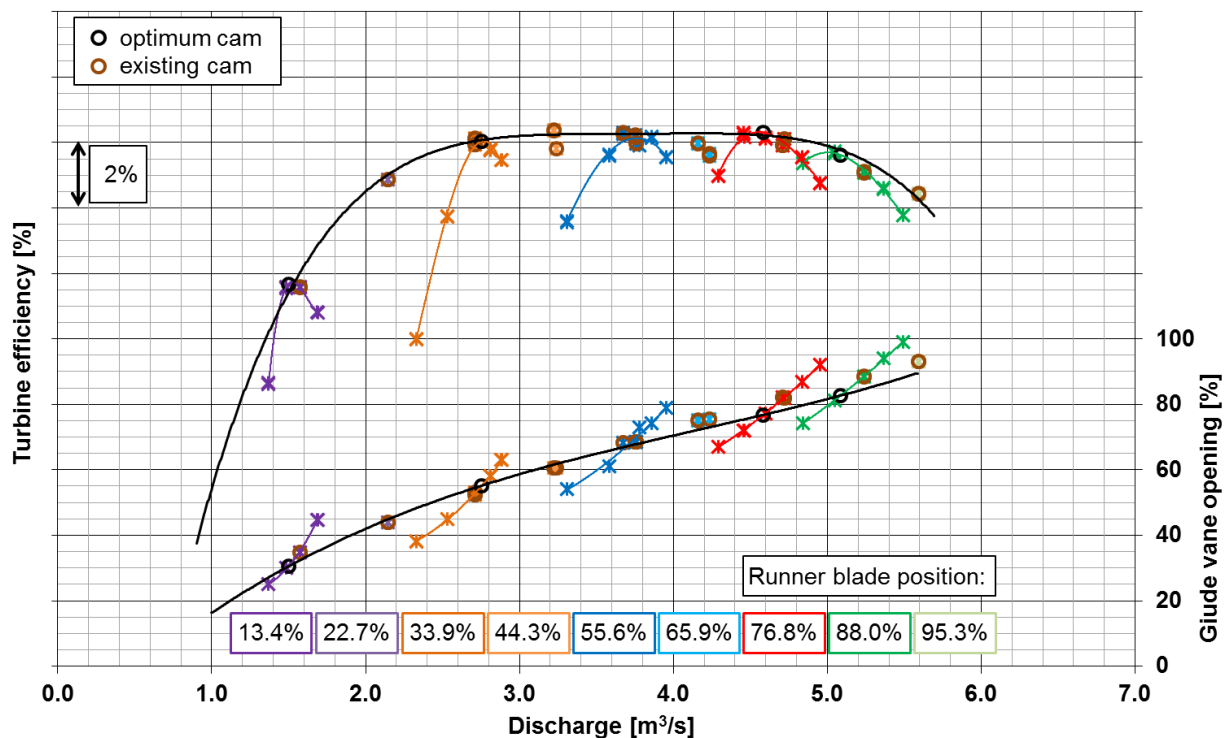


Figure 13. Turbine efficiency and cam correlation for MG 1 at the dotation HPP Pradella.

7. Conclusions

Efficiency and cam correlation tests were successfully performed with the ATT discharge measurements. Propeller curves were determined for the two machine groups over the operating range of interest. The on-cam points and their resulting efficiencies lie well on the optimum envelope. The determined relation of blade opening with the measured discharge allows the operator to determine the discharge through the turbines and to provide the contractual residual water in the river downstream of the weir.

Due to the crossed path arrangement a rotation of the flow in the channel could be analyzed. The ratio of the transversal to the mean axial velocity amounts up to 25 %. The reason for the rotating flow can be explained with the geometry of the intake structure to the open channel and the successive bend. An ATT installation without crossed paths would result in a mean under- or overestimation of 1.4 % of the discharge in the presented case study.

Furthermore, an unusual axial velocity flow profile was observed. The highest velocity was measured close to the channel bottom. This makes the extrapolation to the channel bottom critical. A graphical based estimation was the only way to compare different numbers of the bottom coefficient (area-ratios). Errors of up to 0.75 % or more can easily be introduced by choosing bottom coefficients, which are not physical for the flow profile found in the presented study.

Low frequency fluctuations were found analyzing the measured signals. Such fluctuations are typical for turbulent flows but in the present case the energy content was high due to the pronounced inlet swirl. These, more or less stochastically varying, low frequency components demanded longer acquisition durations.

Acknowledgment

The authors would like to express their gratitude to the company Engadiner Kraftwerke AG and his staff involved in the dotation hydro power plant operation and supervision during the test at Pradella.

References

1. IEC Standard 60041 (1991). Field acceptance tests to determine the hydraulic performance of hydraulic turbines, storage pumps and pump-turbines, *IEC*, 3rd edition, Geneva, Switzerland.
2. Lanzersdorfer J (2012). Discharge measurements at Chievo Dam power plant using 24 ultrasonic paths, *Proc. 9th Intl. Conference on Hydraulic Efficiency Measurements*, IGHEM, Trondheim, Norway.
3. Hug S, Staubli T and Gruber P (2012). Comparison of measured path velocities with numerical simulations for heavily disturbed velocity distributions, *Proc. 9th Intl. Conference on Hydraulic Efficiency Measurements*, IGHEM, Trondheim, Norway.
4. ISO Standard 6416 (2004). Hydrometry – Measurement of discharge by the ultrasonic (acoustic) method, *IEC*, 3rd edition, Geneva, Switzerland.
5. ISO Standard 748 (2007). Hydrometry – Measurement of liquid flow in open channels using current-meters or floats, *IEC*, 4th edition, Geneva, Switzerland.
6. Giordano P (1995). Il calcolo della portata nei canali a pelo libero a partire da misure di velocità media trasversale, *ENEL*, Italy.
7. Blanckaert K (2003). Flow and turbulence in sharp open-channel bends, *PhD thesis* no. 2545, EPFL, Lausanne, Switzerland.
8. IEC Standard 62006 (2010). Hydraulic machines – Acceptance tests of small hydroelectric installations, *IEC*, 1st edition, Geneva, Switzerland.

Authors

André Abgottspon graduated in Mechanical Engineering (M.Sc.) from the Hochschule Luzern in Horw. Since 2006 he works as a research associate in the university's Competence Center Fluid Mechanics and Hydro Machines, e.g. in the fields of hydro power plant efficiency measurements, Pelton jet quality and hydro-abrasive erosion. In 2009 he co-founded etaeval GmbH, a company specialized in measurements, simulations and monitorings on hydro power plants.

Prof. Dr. Thomas Staubli graduated in Mechanical Engineering from the Swiss Federal Institute of Technology (ETH) in Zürich. After two years of post-doctoral research in the field of flow induced vibration at Lehigh University, Pennsylvania, he worked in experimental fluid mechanics at Sulzer Hydro (now Andritz Hydro) in Zürich. He then headed the Hydro Machinery Laboratory at the ETH Zürich. During this period he directed research projects in the field of hydraulic machinery. Since 1996 he is professor for Fluid Mechanics and Hydro Machines at the Hochschule Luzern.

Nicolas Gloor graduated in Wood Engineering (B.Sc.) from the Berne University of Applied Sciences. After his graduation he worked four years in the wood industry as a process engineer. Since 2015 he is undergoing his second graduation in Mechanical Engineering at the Hochschule Luzern. Also since 2015 he works for etaeval.